

# 支柱持圓形懸掛式平板之研究

劉富理

本論文是研究由同一環等矩離柱子所支持之圓形懸掛式平板，研究之基本假設是該環柱子反力不承受彎矩及為一沿環之綫型均勻分佈力，為了設計此種結構之方便，本論文做一些參變數之研究，其結果以圓形曲線劃出，以備參考。

---

## A B S T R A C T

A complete solution for the bending of an overhanging full circular plate supported on a ring of equally spaced columns is presented. The problem is solved under the assumptions that the columns do not restrain the rotation of the slab, and that the column reaction is a uniformly distributed line load along the ring. Some limiting cases are investigated and parametric studies are carried out. The results are presented in the form of charts to facilitate the analysis and the design of such structures.

## TABLE OF CONTENTS

<b>CHAPTER</b>	<b>TITLE</b>	<b>PAGE</b>
	Abstract	115
	Table of Contents	116
	List of Figures	117
	List of Symbols	118
I	INTRODUCTION	119
II	METHOD OF ANALYSIS	120
	Assumptions	120
	Governing Equations	120
	Boundary and Continuity Conditions	120
	Stress Resultants	122
III	LIMITING CASES	124
IV	PARAMETRIC STUDIES AND CONCLUSIONS	125
	REFERENCES	126

## LIST OF FIGURES

<b>FIGURE</b>	<b>TITLE</b>	<b>PAGE</b>
1	Full Circular Plate Supported on k Equally Spaced Columns	127
2	Deflection $w$ Versus Dimensionless Radius $\rho$ for $k=4$ , $\nu_1=\nu_2=0.2$ , $D_1=D_2=D$ and $\alpha=\pi/64$	128
3	Deflection $w$ Versus Dimensionless Radius $\rho$ for $k=8$ , $\nu_1=\nu_2=0.2$ , $D_1=D_2=D$ and $\alpha=\pi/64$	129
4	Deflection $w$ Versus Dimensionless Radius $\rho$ for $k=16$ , $\nu_1=\nu_2=0.2$ , $D_1=D_2=D$ and $\alpha=\pi/64$	130
5	Deflection $w$ Versus Dimensionless Radius $\rho$ for $k=64$ , $\nu_1=\nu_2=0.2$ , $D_1=D_2=D$ and $\alpha=\pi/64$	131
6	Radial Moment $M_r$ Versus Dimensionless Radius $\rho$ for $k=4$ , $\nu_1=\nu_2=0.2$ , $D_1=D_2=D$ and $\alpha=\pi/64$	132
7	Radial Moment $M_r$ Versus Dimensionless Radius $\rho$ for $k=8$ , $\nu_1=\nu_2=0.2$ , $D_1=D_2=D$ and $\alpha=\pi/64$	133
8	Radial Moment $M_r$ Versus Dimensionless Radius $\rho$ for $k=16$ , $\nu_1=\nu_2=0.2$ , $D_1=D_2=D$ and $\alpha=\pi/64$	134
9	Radial Moment $M_r$ Versus Dimensionless Radius $\rho$ for $k=64$ , $\nu_1=\nu_2=0.2$ , $D_1=D_2=D$ and $\alpha=\pi/64$	135
10	Radial Shear $Q_r$ Versus Dimensionless Radius $\rho$ for $k=4$ , $\nu_1=\nu_2=0.2$ , $D_1=D_2=D$ and $\alpha=\pi/64$	136
11	Radial Shear $Q_r$ Versus Dimensionless Radius $\rho$ for $k=8$ , $\nu_1=\nu_2=0.2$ , $D_1=D_2=D$ and $\alpha=\pi/64$	137
12	Radial Shear $Q_r$ Versus Dimensionless Radius $\rho$ for $k=16$ , $\nu_1=\nu_2=0.2$ , $D_1=D_2=D$ and $\alpha=\pi/64$	138
13	Radial Shear $Q_r$ Versus Dimensionless Radius $\rho$ for $k=64$ , $\nu_1=\nu_2=0.2$ , $D_1=D_2=D$ and $\alpha=\pi/64$	139
14	Transverse Moment $M_\theta$ Versus Angle $\theta$ for $k=4$ , $\nu_1=\nu_2=0.2$ , $D_1=D_2=D$ and $\alpha=\pi/64$	140
15	Transverse Moment $M_\theta$ Versus Angle $\theta$ for $k=8$ , $\nu_1=\nu_2=0.2$ , $D_1=D_2=D$ and $\alpha=\pi/64$	141
16	Transverse Moment $M_\theta$ Versus Angle $\theta$ for $k=16$ , $\nu_1=\nu_2=0.2$ , $D_1=D_2=D$ and $\alpha=\pi/64$	142
17	Transverse Moment $M_\theta$ Versus Dimensionless Radius $\rho$ for $k=64$ , $\nu_1=\nu_2=0.2$ , $D_1=D_2=D$ and $\alpha=\pi/64$	143
18	Transverse Shear $Q_\theta$ Versus Angle $\theta$ for $k=4$ , $\nu_1=\nu_2=0.2$ , $D_1=D_2=D$ and $\alpha=\pi/64$	144
19	Transverse Shear $Q_\theta$ Versus Angle $\theta$ for $k=8$ , $\nu_1=\nu_2=0.2$ , $D_1=D_2=D$ and $\alpha=\pi/64$	145
20	Transverse Shear $Q_\theta$ Versus Angle $\theta$ for $k=16$ , $\nu_1=\nu_2=0.2$ , $D_1=D_2=D$ and $\alpha=\pi/64$	146

## LIST OF SYMBOLS

The following symbols are used:

$a$	= outer radius of slab
$b$	= inner radius of slab
$C', E', C, E, F, G$	= integration constants
$D, D_1, D_2$	= flexural rigidities of slab
$k$	= number of ring columns
$M_r, M_{r1}, M_{r2}$	= radial bending moments per unit width of section
$M_\theta, M_{\theta1}, M_{\theta2}$	= transverse bending moments per unit width of section
$n$	= summation index
$Q_r, Q_{r1}, Q_{r2}$	= radial shearing forces per unit width of section
$Q_\theta, Q_{\theta1}, Q_{\theta2}$	= transverse shearing forces per unit width of section
$q, q_1, q_2$	= intensity of transverse loads
$r$	= polar radius
$V_r, V_{r1}, V_{r2}$	= supplemented (Kirchhoff) shearing forces per unit width of section
$w, w_1, w_2$	= deflections of slab
$2\alpha$	= central angle subtended by column width
$\beta$	= $b/a$
$\gamma$	= $q_2/q_1$
$\lambda$	= $D_2/D_1$
$\theta$	= polar angle
$\nu, \nu_1, \nu_2$	= Poisson's ratios
$\rho$	= dimensionless radius, $r/a$

The subscripts 1 and 2 refer to the inner and outer domains respectively..

## I INTRODUCTION

Many structural elements such as circular building slabs and circular footings can be treated as circular plates. The analysis of circular plates supported on columns has received some attention because of their practical application in flat plate construction. A full circular plate supported by uniformly distributed reactions over finite arcs of its boundary and subjected to uniformly distributed transverse load was analyzed by GIRKMANN (1959). Annular slabs supported by equally spaced columns along the outer boundary or the inner boundary or the combination of both were treated by AGABEIN, LEE and DUNDURS (1967). The solution to an annular slab fixed at the inner boundary, supported by equally spaced columns along the outer boundary and subjected to uniformly distributed transverse load was presented by KOSHERICK, DUNDURS and LEE (1968).

In this study, a circular plate free on the outer boundary, supported by a ring of equally spaced columns and subjected to uniformly distributed transverse load is investigated.

## II METHOD OF ANALYSIS

Figure 1 depicts the coordinate system and significant dimensions of a full circular plate of radius  $a$  supported on  $k$  equally spaced columns arranged along a circle of radius  $b$ . The plate is divided into two domains with distinct flexural properties and loading intensities. The width of each column is taken as  $2\alpha b$ , so that a column subtends a central angle equal to  $2\alpha$ .

### *Assumptions*

The following assumptions are made to simplify the problem for mathematical treatment. The columns offer no restraint against the rotation of the slab. The force exerted on the slab by each column is a line force uniformly distributed over the width of the column. In view of Saint-Venant's principle, this last assumption should not be very critical provided that the widths of the columns are small in comparison to the size of the slab.

## *Governing Equations*

The middle plane deflection of the slab must satisfy the plate equations

$$\nabla^4 w_1 = q_1 / D_1 \quad (1)$$

$$\nabla^4 w_2 = q_2 / D_2 \quad (2)$$

where  $\nabla^4$  denotes the Laplace operator  $\nabla^2$  applied twice,  $w$ ,  $q$  and  $D$  are the deflection, the load intensity and the flexural rigidity respectively, and the subscripts 1 and 2 refer to the inner and outer domains respectively,

In polar coordinates,

$$\nabla^2 = \frac{\partial^2}{\partial r^2} + \frac{1}{r} \frac{\partial}{\partial r} + \frac{1}{r^2} \frac{\partial^2}{\partial \theta^2} \quad (3)$$

in which  $r$  and  $\theta$  are the polar radius and angle respectively. For equally spaced columns, the slab deflects symmetrically with respect to any diameter bisecting a column. Therefore the deflection functions must be even in  $\theta$ .

Introducing the dimensionless radius  $\rho = r/a$ , the solutions of Eqs. 1 and 2 can be taken in the form

$$w_1 = \frac{q_1 a^4}{64 D_1} [ \rho^4 + C_0' + E_0' \rho^2 + (C_1' \rho + E_1' \rho^3) \cos\theta + \sum_{n=2}^{\infty} (C_n' \rho^n + E_n' \rho^{n+2}) \cos n\theta ] \quad \dots \dots \dots (4)$$

$$w_2 = \frac{q_2 a^4}{64 D_2} [ \rho^4 + C_0 + E_0 \rho^2 + F_0 \log \rho + G_0 \rho^2 \log \rho + (C_1 \rho + E_1 \rho^3 + F_1 \rho^{-1} + G_1 \rho \log \rho) \cos \theta + \sum_{n=2}^{\infty} (C_n \rho^n + E_n \rho^{n+2} + F_n \rho^{-n} + G_n \rho^{-n+2}) \cos n\theta ] \dots\dots\dots(5)$$

in which  $C_0'$  to  $E_n'$  and  $C_0$  to  $G_n$  are arbitrary constants which are to be determined from the boundary conditions at  $\rho=1$ , and the continuity conditions at  $\rho=b/a=\beta$ .

### *Boundary and Continuity Conditions*

The boundary conditions at  $\rho=1$  are

$$(M_{r_2})_{\alpha} = 0 \quad (6)$$

$$(V_{r_2})_{\rho=1} = 0 \quad (7)$$

where

In these equations,  $M_r$  and  $V_r$  are the radial moment and supplemented shearing force per unit width of section respectively and  $\nu$  denotes Poisson's ratio.

The continuity conditions at  $\rho = \beta$  are

$${}^{(w_1)}_{\rho = \beta} = {}^{(w_2)}_{\rho = \beta} \quad (10)$$

$$\left(\frac{\partial w_1}{\partial \beta}\right)_{\rho=\beta} = \left(\frac{\partial w_2}{\partial \beta}\right)_{\rho=\beta} \quad (11)$$

$$(M_{r_1})_{\rho=\beta} = (M_{r_2})_{\rho=\beta} \quad (12)$$

$$(V_{r2})_{\rho=\beta} - (V_{r1})_{\rho=\beta} = f(\theta) \quad (13)$$

where  $f(\theta)$  represents the line column reactions per unit length expanded in a Fourier series of the form

$$f(\theta) = \frac{q_1 a}{\beta} [\beta^2(1-\gamma) + \gamma] \left[ \frac{1}{2} + \sum_{n=k, 2k, \dots}^{\infty} \frac{\sin n\alpha}{n\alpha} \cos n\theta \right] \quad (14)$$

where  $\gamma = q_2/q_1$ .

In view of Eq. 14, substituting Eqs. 4 and 5 in Eqs. 6, 7 and 10 to 13 and equating the coefficients of each harmonic lead to three sets of simultaneous equations, the first set involving  $C'_0$ ,  $E'_0$ ,  $C_0$ ,  $E_0$ ,  $F_0$  and  $G_0$ , the second  $C'_1$ ,  $E'_1$ ,  $C_1$ ,  $E_1$ ,  $F_1$  and  $G_1$ , and the third  $C'_n$ ,  $E'_n$ ,  $C_n$ ,  $E_n$ ,  $F_n$  and  $G_n$ . There are five linearly independent equations each in the first two sets and six in the third sets. The two additional conditions needed for the determination of the constants of integration are

$$(\text{w}_1)_{\rho = \beta} = 0 \quad (15)$$

$$, \left( w_1 \right)_{\substack{\rho = \beta \\ \theta = 2\pi/k}}^{\theta = 0} = 0 \quad (16)$$

Finally, solving Eqs. 6, 7, 10 to 13, 15 and 16 for the constants yields

$$C_0 = -\frac{\lambda}{\beta'}(S_1 + E'_0 \beta^2 + 2\beta^4) + \beta^2(\beta^2 - 4) + F_0 \left( \frac{1}{2} - \log \beta \right) \quad (17)$$

$$C_0' = -(S_1 + E_0 \beta^2 + \beta^4) \quad (18)$$

$$E_0 = 4(1+2\log \beta) - 2\beta^2 \left(1 - \frac{\lambda}{\gamma'}\right) + \frac{\lambda}{\gamma'} E'_0 - \frac{1}{2} F_0 \beta^{-2} \quad (19)$$

$$E_0' = -\frac{2\gamma}{\lambda} \frac{1}{M_1} [P(1 + \frac{1-\nu_3}{1+\nu_3} \beta^2) - Q(1 + \frac{1-\nu_2}{1+\nu_2})] \quad (20)$$

$$F_0 = -4\beta^2 \frac{1}{M_1} [P - Q (1 - \frac{1}{\lambda} \frac{1 + \nu_1}{1 + \nu_2})] \quad (21)$$

$$G_0 = -8 \quad (22)$$

where

$$S_1 = \sum_{n=1}^{\infty} \beta^n (C_n + E_n \beta^{-2}) \quad (23)$$

$$P = \frac{4}{1+\nu_2} - \beta^2 \left[ \frac{2}{1+\nu_2} + \frac{\lambda}{\gamma} \left( 1 - \frac{1}{\lambda} \frac{3+\nu_1}{1+\nu_2} \right) \right] \quad (24)$$

$$Q = \frac{1-\nu_2}{1+\nu_2} + \left( 1 - \frac{\lambda}{\gamma} \right) \beta^2 - 4 \log \beta \quad (25)$$

$$M_1 = \frac{1-\nu_2}{1+\nu_2} (1 - \beta^2) + \frac{1}{\lambda} \frac{1+\nu_1}{1+\nu_2} \left( 1 + \frac{1-\nu_2}{1+\nu_2} \beta^2 \right) \quad (26)$$

Furthermore,

$$C'_1 = E'_1 = C_1 = E_1 = F_1 = G_1 = 0 \quad (27)$$

Finally, for  $n=k, 2k, \dots$ ,

$$C_n = \frac{1}{n(n-1)} \frac{N}{M_2} \beta^2 [\mu_1 A + (n-1)B \beta^{-2n} - \mu_2 H \beta^{-2n-2}] \quad (28)$$

$$C'_n = \frac{1}{n(n-1)} \frac{N}{M_2} \frac{\gamma}{\lambda} \beta^2 \{ A R + (1+\mu_1) \beta^{-2n} [n(n-1) - H \beta^{-2} - n \mu_1 \beta^{2n}] \} \quad (29)$$

$$E_n = -\frac{1}{n+1} \frac{N}{M_2} [\mu_1 \mu_3 + B \beta^{-2n+2} - (n+1) \mu_2 \beta^{-2n}] \quad (30)$$

$$E'_n = -\frac{1}{n+1} \frac{N}{M_2} \frac{\gamma}{\lambda} \{ \mu_3 R + (1+\mu_1) \beta^{-2n+2} [n - (n+1) \beta^{-2} - \mu_1 \beta^{-2n-2}] \} \quad (31)$$

$$F_n = \frac{1}{n(n+1)} \frac{N}{M_2} \beta^2 [-(n+1)A + \mu_3 H \beta^{-2} + \mu_1 B \beta^{-2n}] \quad (32)$$

$$G_n = -\frac{1}{n-1} \frac{N}{M_2} \beta^2 [-A + (n-1) \mu_3 \beta^{-2} + \mu_1 \mu_2 \beta^{-2n-2}] \quad (33)$$

in which

$$\mu_1 = \frac{3+\nu_2}{1-\nu_2}, \mu_2 = 1 + \frac{1}{\lambda} \frac{3+\nu_1}{1-\nu_2}, \mu_3 = 1 - \frac{1}{\lambda} \frac{1-\nu_1}{1-\nu_2}, \mu_4 = 2 \left( \frac{1+\nu_2}{1-\nu_2} - \frac{1}{\lambda} \frac{1+\nu_1}{1-\nu_2} \right) \quad (34)$$

$$A = n \mu_3 + \mu_4 \quad (35)$$

$$B = n \mu_2 - \mu_4 \quad (36)$$

$$H = n^2 - 1 + \mu_1^2 \quad (37)$$

$$R = \mu_1 (1 - \beta^{-2n})^2 + [(n^2 - 1)(1 - \beta^2)^2 + (\beta^2 + \mu_1)^2] \beta^{-2n-2} \quad (38)$$

$$N = 8(1+\mu_1) \frac{\beta^{-n}}{\gamma} [\beta^2(1-\gamma) + \gamma] \frac{\sin n\alpha}{n^2 \alpha} \quad (39)$$

$$M_2 = [(1+\mu_1) - \mu_2 (1 + \mu_1 \beta^{-2n-2})] [\mu_3 (\mu_1 + \beta^{-2n+2}) - (1+\mu_1) \beta^{-2n+2}] \\ - (n^2 - 1) \mu_2 \mu_3 (1 - \beta^2)^2 \beta^{-2n-2} \quad (40)$$

### Stress Resultants

In view of the foregoing the deflection functions, Eqs. 4 and 5, and the stress resultants take following forms. For the inner domain,

$$\frac{w_1 D_1}{q_1 a^4} = \frac{1}{64} [\rho^4 + C'_0 + E'_0 \rho^2 + \sum_{n=k, 2k, \dots}^{\infty} (C'_n \rho^n + E'_n \rho^{n+2}) \cos n\theta] \quad (41)$$

$$\frac{M_{r1}}{q_1 a^2} = -\frac{1-\nu_2}{64} \{ 4 \frac{3+\nu_1}{1-\nu_2} \rho^2 + 2 \frac{1+\nu_1}{1-\nu_2} E'_0 + \sum_{n=k, 2k, \dots}^{\infty} [n(n-1) \frac{1-\nu_1}{1-\nu_2} C'_n \rho^{n-2} \\ + (n+1) (\frac{1-\nu_1}{1-\nu_2} + 2 \frac{1+\nu_1}{1-\nu_2}) E'_n \rho^n] \cos n\theta \} \quad (42)$$

$$\frac{Q_{r1}}{q_1 a} = -\frac{1}{16} \sum_{n=k, 2k, \dots}^{\infty} [8\rho + n(n+1) E'_n \rho^{n-1} \cos n\theta] \quad (43)$$

$$\begin{aligned} \frac{M_{\theta 1}}{q_1 a^2} = & -\frac{1-\nu_2}{64} \left\{ 4 \frac{1+3\nu_1}{1-\nu_2} \rho^2 + 2 \frac{1+\nu_1}{1-\nu_2} E'_0 - \sum_{n=k, 2k, \dots}^{\infty} [n(n-1) \frac{1-\nu_1}{1-\nu_2} C'_n \rho^{n-2} \right. \\ & \left. + (n^2 \frac{1-\nu_1}{1-\nu_2} - n \frac{1+3\nu_1}{1-\nu_2} - 2 \frac{1+\nu_1}{1-\nu_2}) E'_n \rho^n] \cos n\theta \right\} \end{aligned} \quad (44)$$

$$\frac{Q_{\theta 1}}{q_1 a} = \frac{1}{16} \sum_{n=k, 2k, \dots}^{\infty} n(n+1) E'_n \rho^{n-1} \sin n\theta \quad (45)$$

and for the outer domain,

$$\begin{aligned} \frac{w_2 D_2}{q_2 a^4} = & \frac{1}{64} [\rho^4 + C_0 + E_0 \rho^2 + F_0 \log \rho + G_0 \rho \log^2 \rho + \sum_{n=k, 2k, \dots}^{\infty} (C_n \rho^n + E_n \rho^{n+2} \\ & + F_n \rho^{-n} + G_n \rho^{-n+2}) \cos n\theta] \end{aligned} \quad (46)$$

$$\begin{aligned} \frac{M_{r2}}{q_2 a^2} = & -\frac{1-\nu_2}{64} \left\{ 4 \frac{3+\nu_2}{1-\nu_2} \rho^2 + 2 \frac{1+\nu_2}{1-\nu_2} E_0 - F_0 \rho^{-2} + G_0 \left( \frac{3+\nu_2}{1-\nu_2} + 2 \frac{1+\nu_2}{1-\nu_2} \log \rho \right) \right. \\ & + \sum_{n=k, 2k, \dots}^{\infty} [n(n-1) C_n \rho^{n-2} + (n+1) (n+2) \frac{1+\nu_2}{1-\nu_2} E_n \rho^n + n(n+1) F_n \rho^{-n-2} \\ & \left. + (n-1) (n-2) \frac{1+\nu_2}{1-\nu_2} G_n \rho^{-n}] \cos n\theta \right\} \end{aligned} \quad (47)$$

$$\frac{Q_{r2}}{q_2 a} = -\frac{1}{16} \left\{ 8\rho + G_0 \rho^{-1} + \sum_{n=k, 2k, \dots}^{\infty} [n(n+1) E_n \rho^{n-1} + n(n-1) G_n \rho^{-n+1}] \cos n\theta \right\} \quad (48)$$

$$\begin{aligned} \frac{M_{\theta 2}}{q_2 a^2} = & -\frac{1-\nu_2}{64} \left\{ 4 \frac{1+3\nu_2}{1-\nu_2} \rho^2 + 2 \frac{1+\nu_2}{1-\nu_2} E_0 + F_0 \rho^{-2} + G_0 \left( \frac{1+3\nu_2}{1-\nu_2} + 2 \frac{1+\nu_2}{1-\nu_2} \log \rho \right) \right. \\ & - \sum_{n=k, 2k, \dots}^{\infty} [n(n-1) C_n \rho^{n-2} + (n^2 - n) \frac{1+3\nu_2}{1-\nu_2} - 2 \frac{1+\nu_2}{1-\nu_2} E_n \rho^n \\ & \left. + n(n-1) F_n \rho^{-n-2} + (n^2 + n) \frac{1+3\nu_2}{1-\nu_2} - 2 \frac{1+\nu_2}{1-\nu_2} G_n \rho^{-n}] \cos n\theta \right\} \end{aligned} \quad (49)$$

$$\frac{Q_{\theta 2}}{q_2 a} = \frac{1}{16} \sum_{n=k, 2k, \dots}^{\infty} n [(n+1) E_n \rho^{n-1} - (n-1) G_n \rho^{-n-1}] \sin n\theta \quad (50)$$

In these equations,  $M_{\theta}$  and  $Q_{\theta}$  are the transverse bending moment and the transverse shearing force per unit width of section respectively. The subscripts 1 and 2 refer to the inner and outer domains respectively.

## III LIMITING CASES

The most immediate limiting case is that of a full circular plate supported by a ring wall. This is obtained by setting  $\alpha = \pi/k$ . The corresponding deflection functions are given by Eqs. 4 and 5 with  $C'_0, E'_0, C_0, E_0, F_0$  and  $G_0$ , as defined by Eqs. 17 to 22, while

$$C'_n = E'_n = C_n = E_n = F_n = G_n = 0 \quad (51)$$

Thus

$$w_1 = \frac{q_1 a^4}{64 D_1} [\rho^4 + C'_0 + E'_0 \rho^2] \quad (52)$$

$$w_2 = \frac{q_2 a^4}{64 D_2} [\rho^4 + C_0 + E_0 \rho^2 + F_0 \log \rho + G_0 \rho^2 \log \rho] \quad (53)$$

Another limiting case is obtained by setting  $\beta \rightarrow 1, \nu_1 = \nu_2 = \nu, q_1 = q_2 = q$  and  $D_1 = D_2 = D$  in Eq. 4. In this case the outer domain vanishes automatically, leading to the solution for a full circular plate supported on columns,

$$w = \frac{qa^4}{64D} \left[ \rho^4 + \frac{5+\nu}{1+\nu} + S_2 - 2 \frac{3+\nu}{1+\nu} \rho^2 + \frac{32}{3+\nu} \sum_{n=k,2k,\dots}^{\infty} (C'_n \rho^n + E'_n \rho^{n+2}) \cos n\theta \right] \quad (54)$$

where

$$S_2 = \frac{64}{(1-\nu)(3+\nu)} \sum_{n=k,2k,\dots}^{\infty} \frac{2n+1+\nu}{n^2(n^2-1)} \frac{\sin n\alpha}{n\alpha} \quad (55)$$

$$C'_n = -\frac{n(1-\nu)+2(1+\nu)}{n^2(n-1)} \frac{\sin n\alpha}{(1-\nu)n\alpha} \quad (56)$$

$$E'_n = \frac{1}{n(n+1)} \frac{\sin (n+2)\alpha}{n\alpha} \quad (57)$$

Note that the solution agrees with that of AGABEIN, et al (1967).

Another interesting case is obtained by setting  $\beta \rightarrow 1, \nu_1 = \nu_2 = \nu, q_1 = q_2 = q$  and  $D_1 = D_2 = D$  in Eq. 52 or by setting  $\alpha = \pi/k$  in Eq. 54. This leads to

$$w = \frac{qa^4}{64D} \left[ \rho^4 - 2 \frac{3+\nu}{1+\nu} \rho^2 + \frac{5+\nu}{1+\nu} \right] \quad (58)$$

which is the deflection of a simply supported and uniformly loaded full circular plate.

Two more cases are encountered when  $\gamma \rightarrow 0$  and  $\gamma \rightarrow \infty$ , which lead to a full circular slab subjected to uniformly distributed load only in the inner domain and the outer domain respectively. Special treatments are needed for these two cases, and the final results are presented together with the case where  $\gamma=1$  in Figs. 2 to 20.

#### IV PARAMETRIC STUDIES AND CONCLUSIONS

For design purpose, the deflection and the stress resultants are plotted against arguments of  $\rho$  for various values of  $\theta$ ,  $\beta$ ,  $\gamma$  and  $k$  in Figs. 2 to 13. The transverse stress resultants are plotted against arguments of  $\theta$  for various values of  $\rho$ ,  $\beta$ ,  $\gamma$  and  $k$  in Figs. 14 to 16 and 18 to 20. In each figure,  $k$  is constant,  $\lambda=1$ ,  $\gamma=1, 0$  and  $\infty$ ,  $\beta=0.5, 0.75$  and  $1$ ,  $\nu_1=\nu_2=0.2$  and  $\alpha=\pi/64$ . The number columns considered are  $k=4, 8, 16$  and  $64$ . Note that  $k=64$  corresponds to a plate supported by a ring wall where  $Q_\theta$  vanishes everywhere and  $M_\theta$  is plotted against arguments of  $\rho$  in Fig. 17. The supplemented shearing force  $V_r$  for  $\beta=1$  and  $\theta=0$ , which is identical to the column reaction is also identified in Figs. 10 to 12. Figs. 2 to 20 show that increasing  $k$  decreases the absolute values of the maximum deflection and stress resultants for particular values of  $\beta$  and  $\gamma$ .

The deflections for  $k=16$  and  $64$  are practically equal, while the bending stress resultants differ slightly for these two values of  $k$  with the exception of the vicinity of the columns. It can be seen from Eqs. 42 and 44 that the values of  $M_r$  and  $M_\theta$  at the center of the plates, for  $k>2$  and particular values of  $\beta$  and  $\gamma$ , are independent of  $k$ . This point can be verified in Figs. 6 to 9 and 14 to 17.

It is obvious that the rate of convergence of the infinite series in the solutions presented increases with increase of the number of columns. An accuracy where the amplitude of the current term is equal to 0.5% of the current sum is achieved in computing the deflection and the stress resultant by using less than ten terms of the series for the most part with the exception of the vicinity of the column support where around twenty terms are needed. The current sum of the series involved is a periodic function of the number of terms in the summation. The shearing forces  $Q_r$  and  $Q_\theta$  have the slowest rate of convergence. The calculation of  $Q_r$  requires the arithmetic mean of the fourth period of the series summation to obtain the same accuracy for  $\rho=\beta$ , where the values are known. The values of  $Q_\theta$  are obtained in the same manner.

REF E R E N C E S

- AGABEIN, M. E., LEE, S. L. and DUNDURS, J. (1967),  
Bending of an Annular Slab Supported on Columns, *Journal of the Franklin Institute*, Vol. 284, No. 5, p. 300.
- GIRKMANN, K. (1959),  
*Klachentrangwerke*, 5th edition, Springer-Verlag, Wein, Austria, P.247.
- KOSHERICK, H. J., DUNDURS, J. and LEE, S. L. (1968),  
Annular Slabs in Circular Core Buildings, *Journal of the Structural Division*, ASCE, No. ST2, P. 471.
- TIMOSHENKO, S. P. and WOINOWSKY-KRIEGER, S. (1959),  
*Theory of Plates and Shells*, 2nd edition, McGraw-Hill Book Co., Inc., New York.

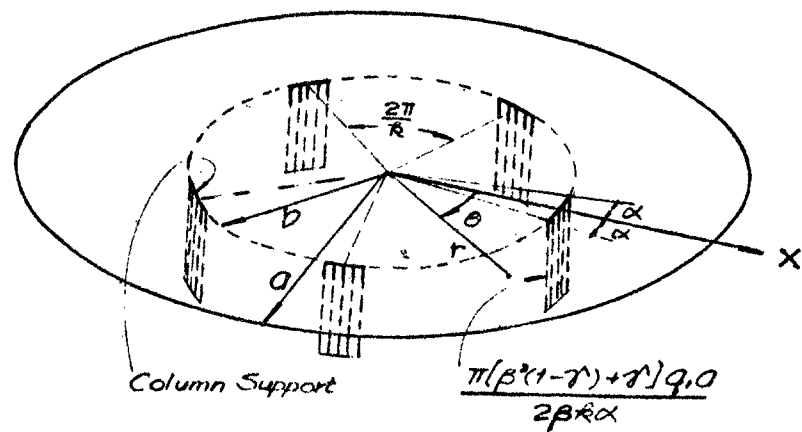


FIG. 1 — FULL CIRCULAR PLATE SUPPORTED ON  
A EQUALLY SPACED COLUMNS

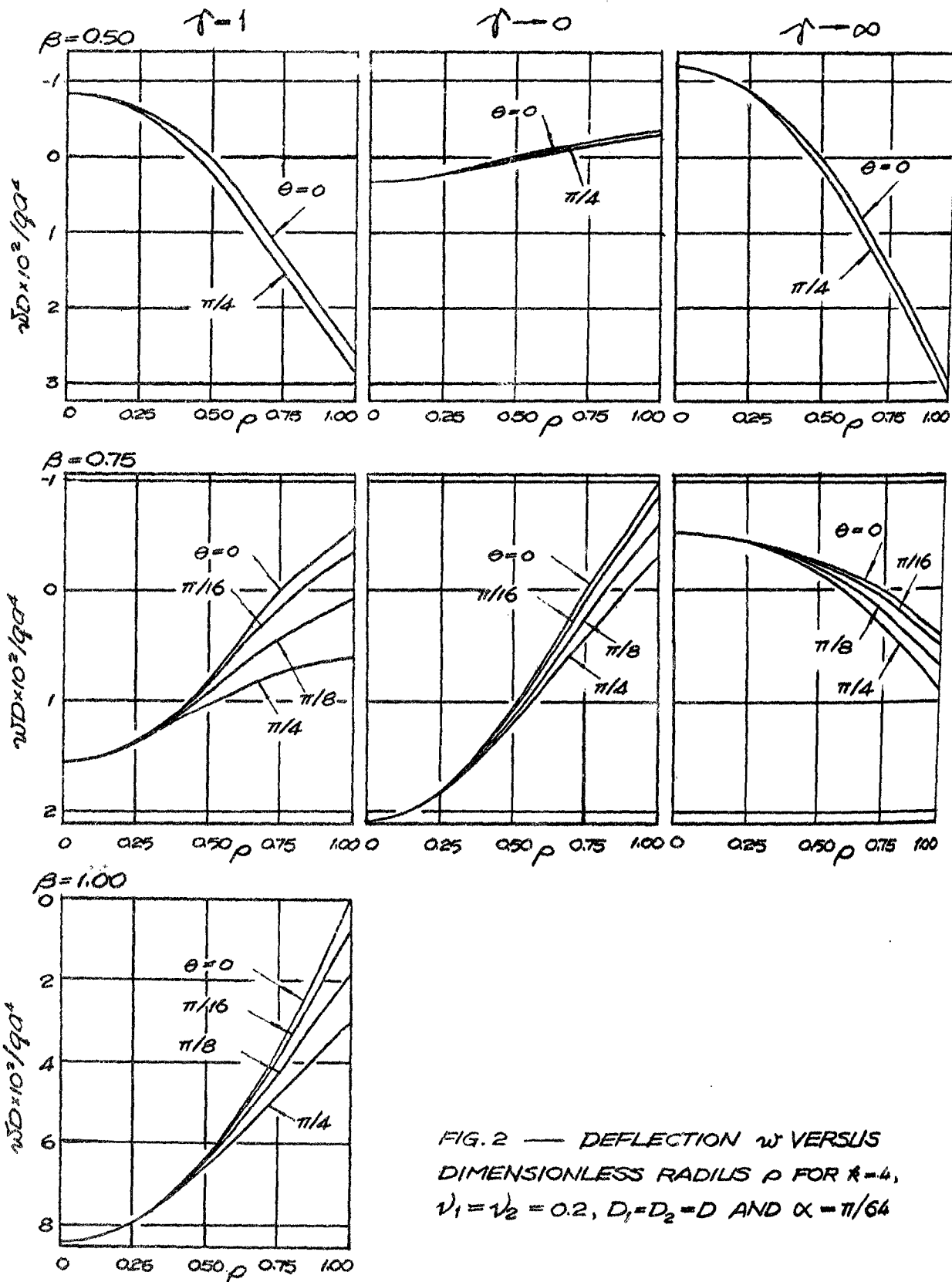


FIG. 2 — DEFLECTION  $w$  VERSUS  
DIMENSIONLESS RADIUS  $\rho$  FOR  $R=4$ ,  
 $V_1=V_2=0.2$ ,  $D_1=D_2=D$  AND  $\alpha=\pi/64$

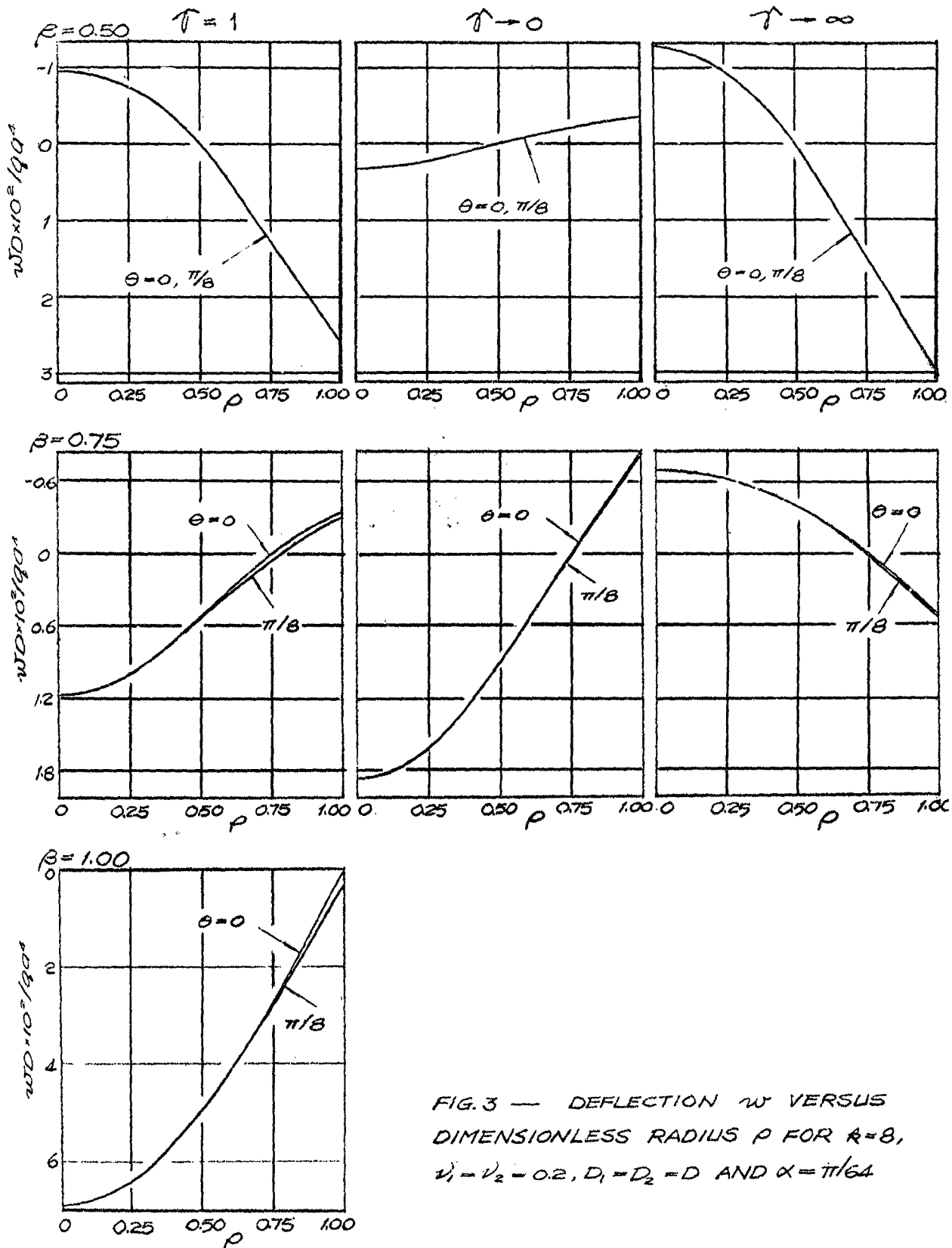


FIG. 3 — DEFLECTION  $w$  VERSUS  
DIMENSIONLESS RADIUS  $\rho$  FOR  $R=8$ ,  
 $\nu_1=\nu_2=0.2$ ,  $D_1=D_2=D$  AND  $\alpha=\pi/64$

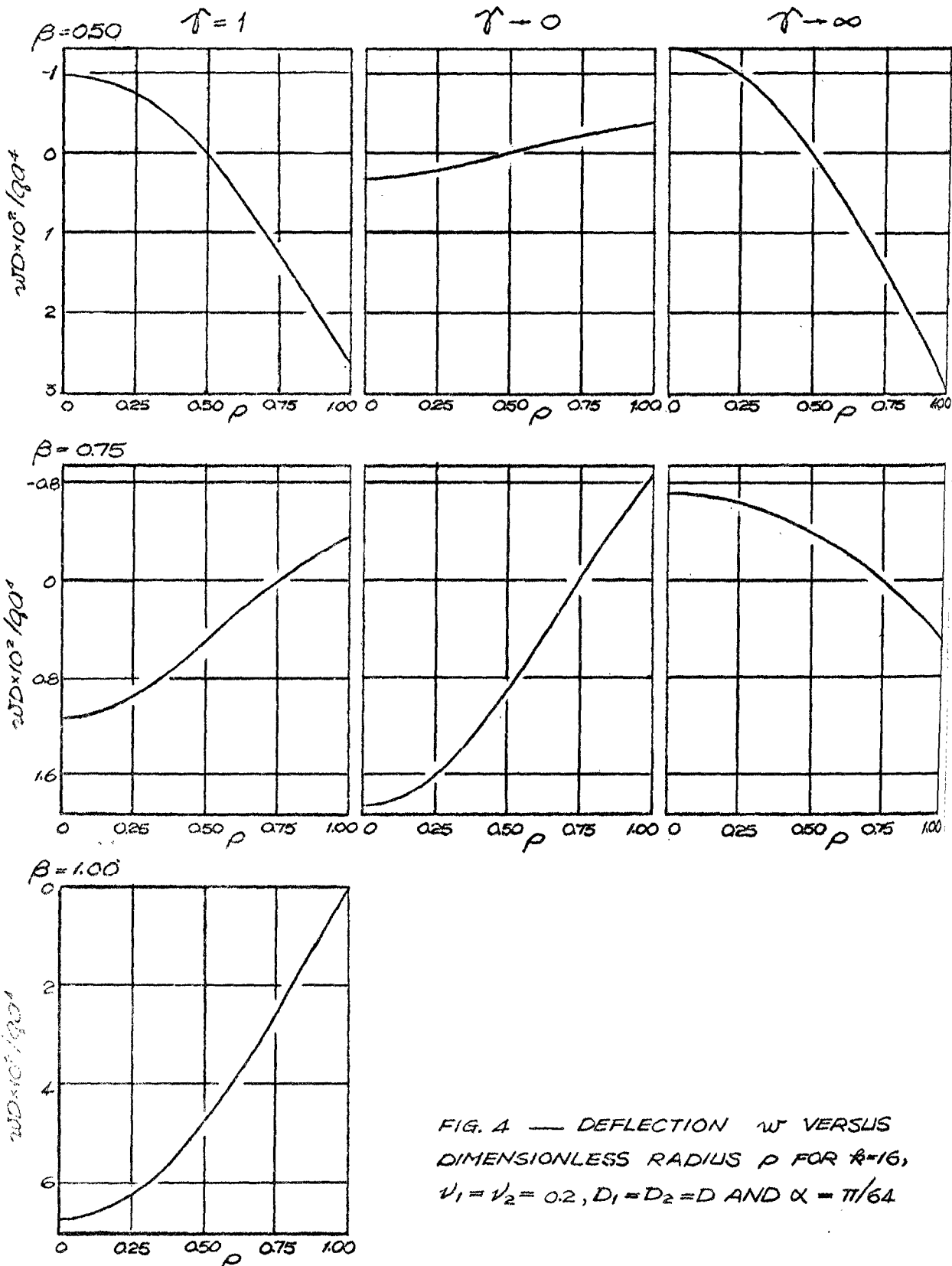
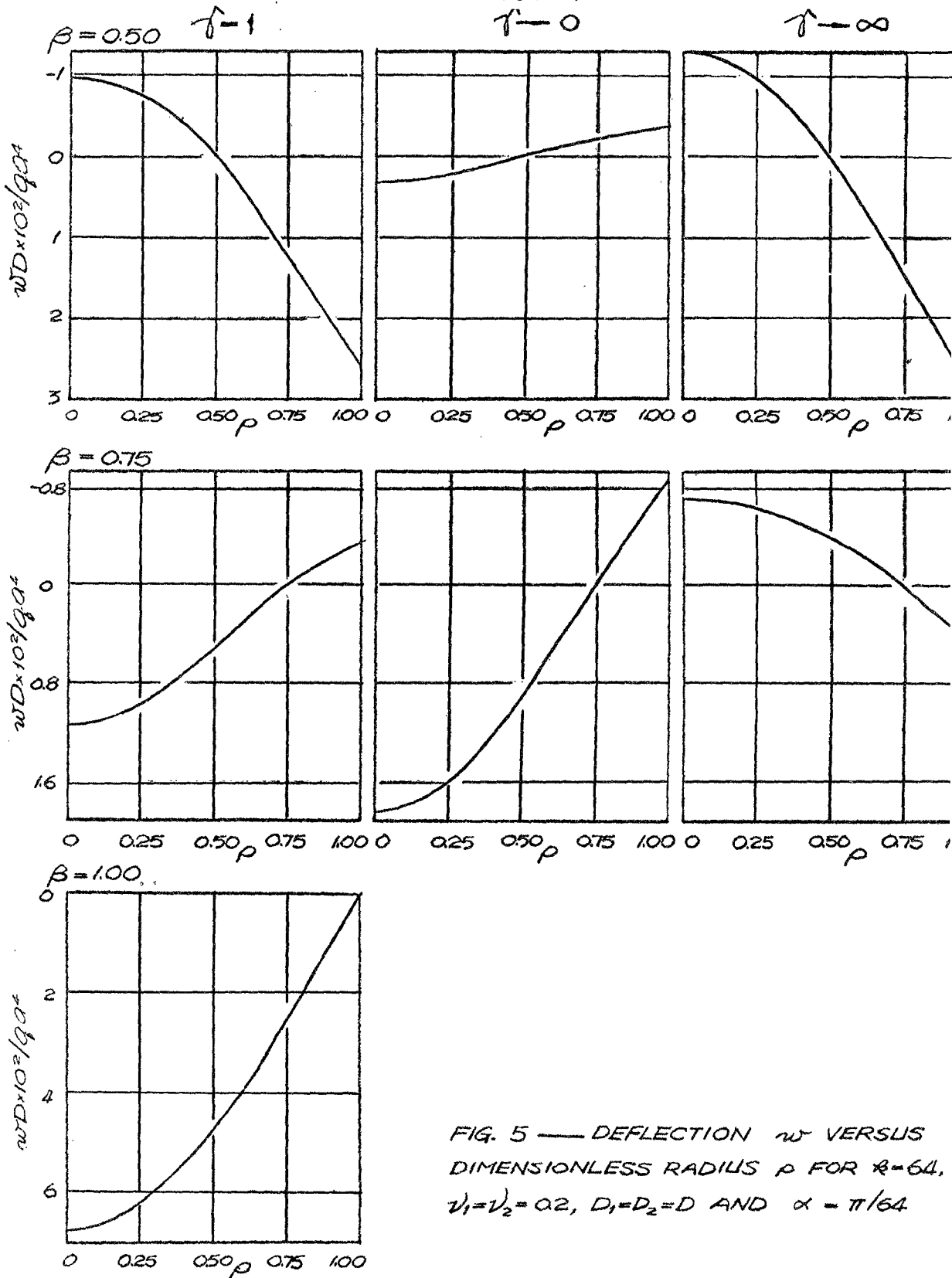


FIG. 4 — DEFLECTION  $w$  VERSUS  
DIMENSIONLESS RADIUS  $\rho$  FOR  $R=16$ ,  
 $\nu_1=\nu_2=0.2$ ,  $D_1=D_2=D$  AND  $\alpha=\pi/64$



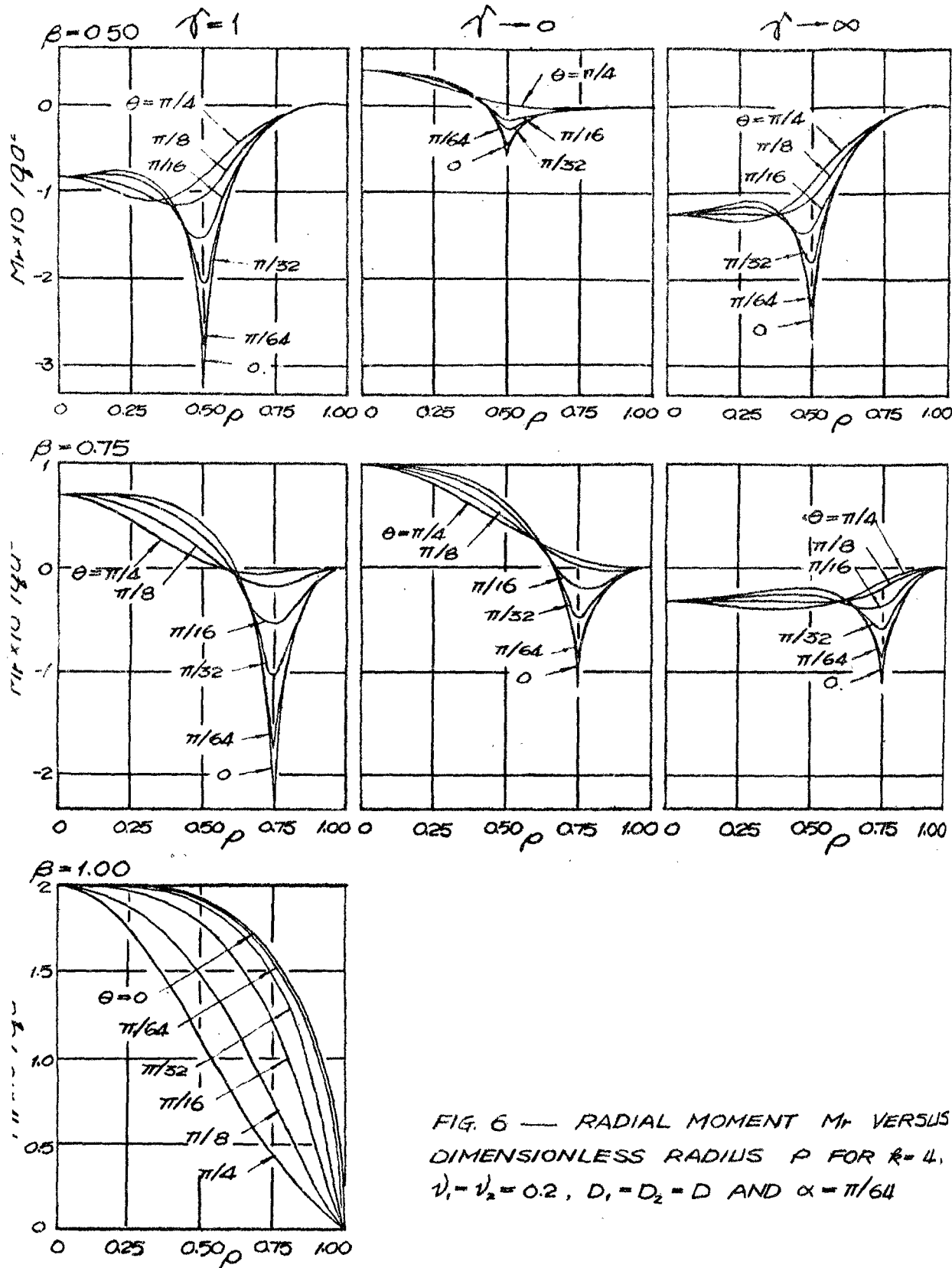


FIG. 6 — RADIAL MOMENT  $M_r$  VERSUS  
DIMENSIONLESS RADIUS  $p$  FOR  $R=4$ ,  
 $\nu_1=\nu_2=0.2$ ,  $D_1=D_2=D$  AND  $\alpha=\pi/64$

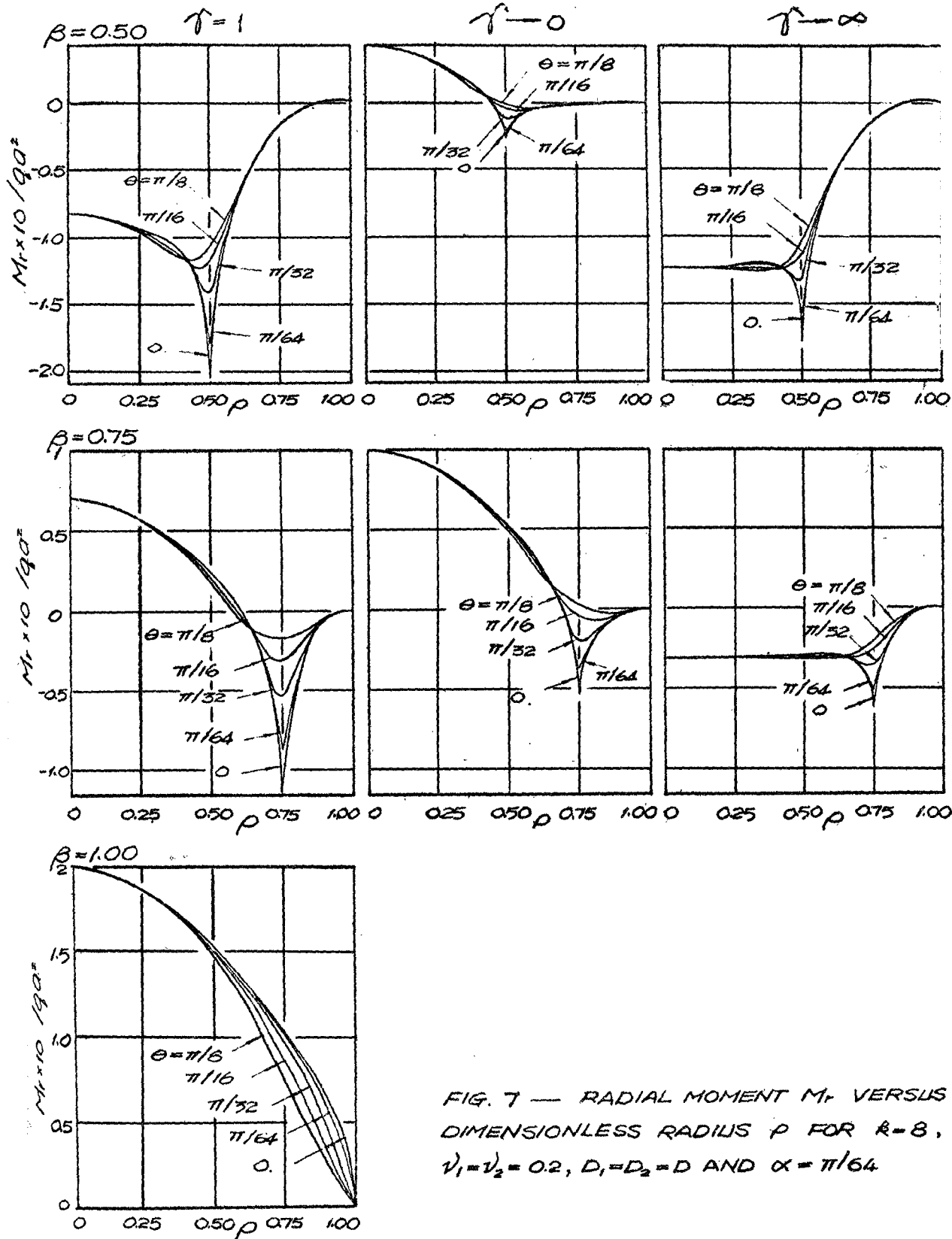


FIG. 7 — RADIAL MOMENT  $M_r$  VERSUS  
DIMENSIONLESS RADIUS  $\rho$  FOR  $R=8$ ,  
 $V_1=V_2=0.2$ ,  $D_1=D_2=D$  AND  $\alpha=\pi/64$

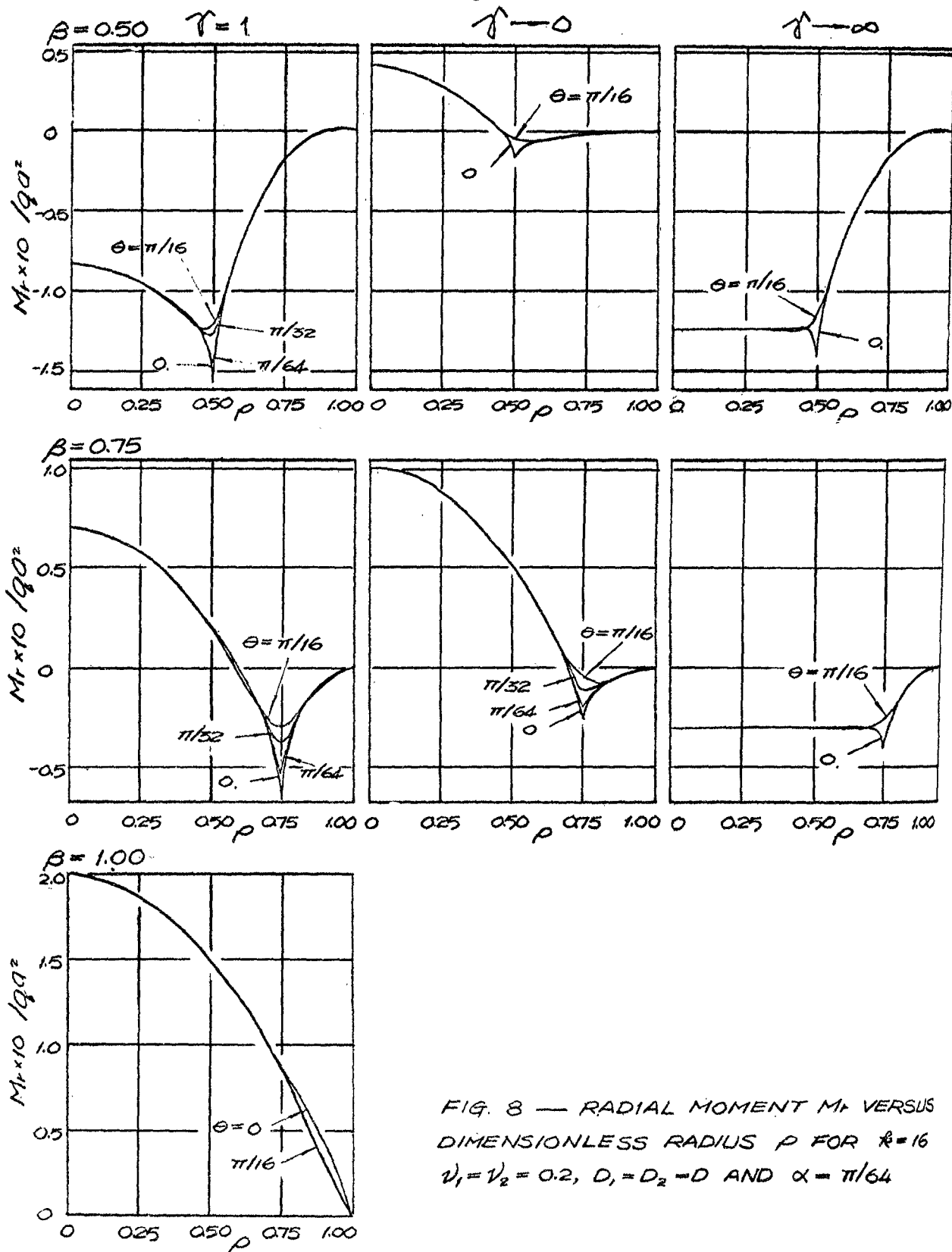


FIG. 8 — RADIAL MOMENT  $M_r$  VERSUS  
DIMENSIONLESS RADIUS  $\rho$  FOR  $R=16$   
 $v_1 = v_2 = 0.2$ ,  $D_1 = D_2 = D$  AND  $\alpha = \pi/64$

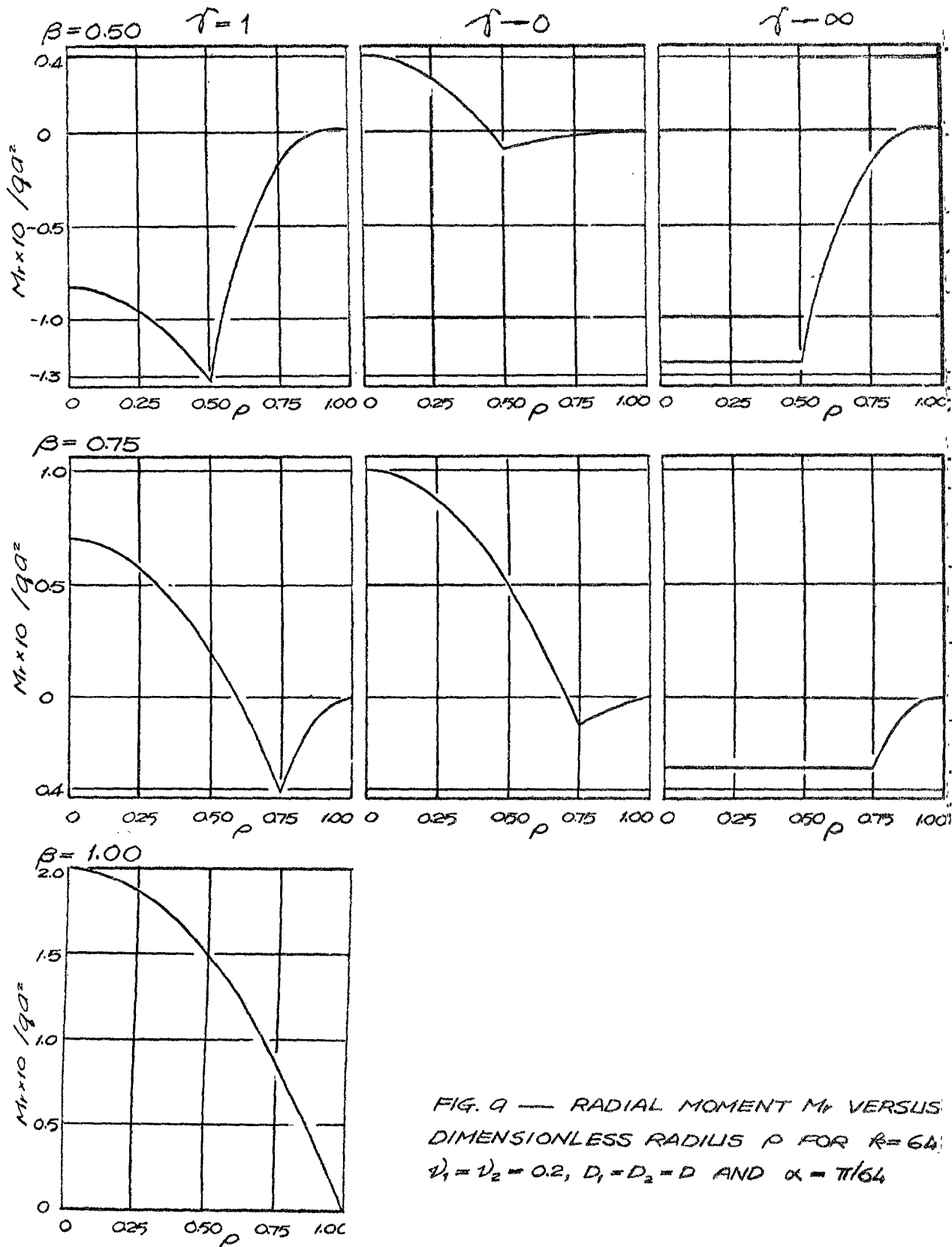


FIG. 9 — RADIAL MOMENT  $M_r$  VERSUS  
DIMENSIONLESS RADIUS  $\rho$  FOR  $R = 64$ ;  
 $\nu_1 = \nu_2 = 0.2$ ,  $D_1 = D_2 = D$  AND  $\alpha = \pi/64$

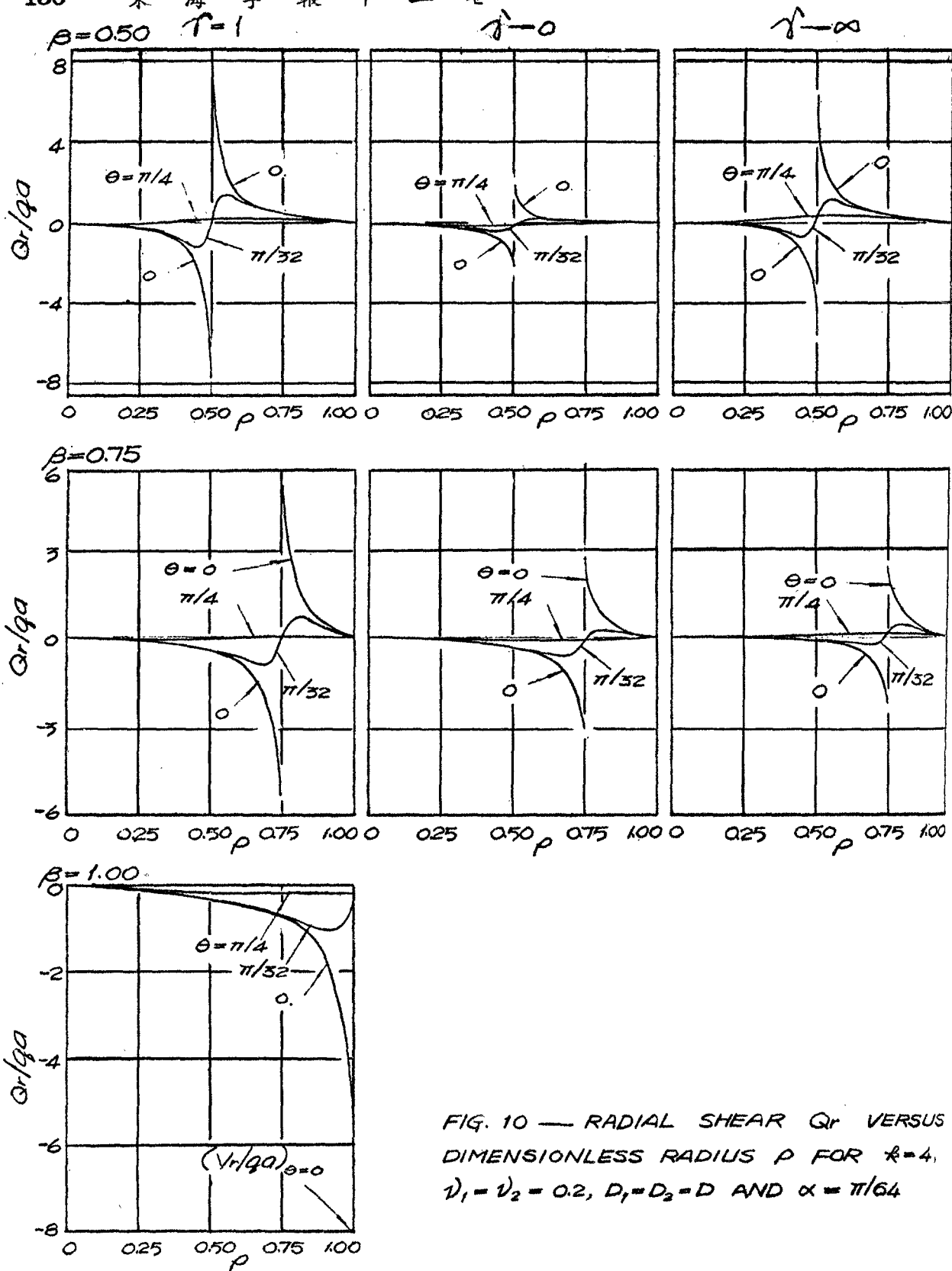


FIG. 10 — RADIAL SHEAR  $Q_r$  VERSUS  
DIMENSIONLESS RADIUS  $\rho$  FOR  $\lambda=4$ ,  
 $\nu_1=\nu_2=0.2$ ,  $D_1=D_2=D$  AND  $\alpha=\pi/64$

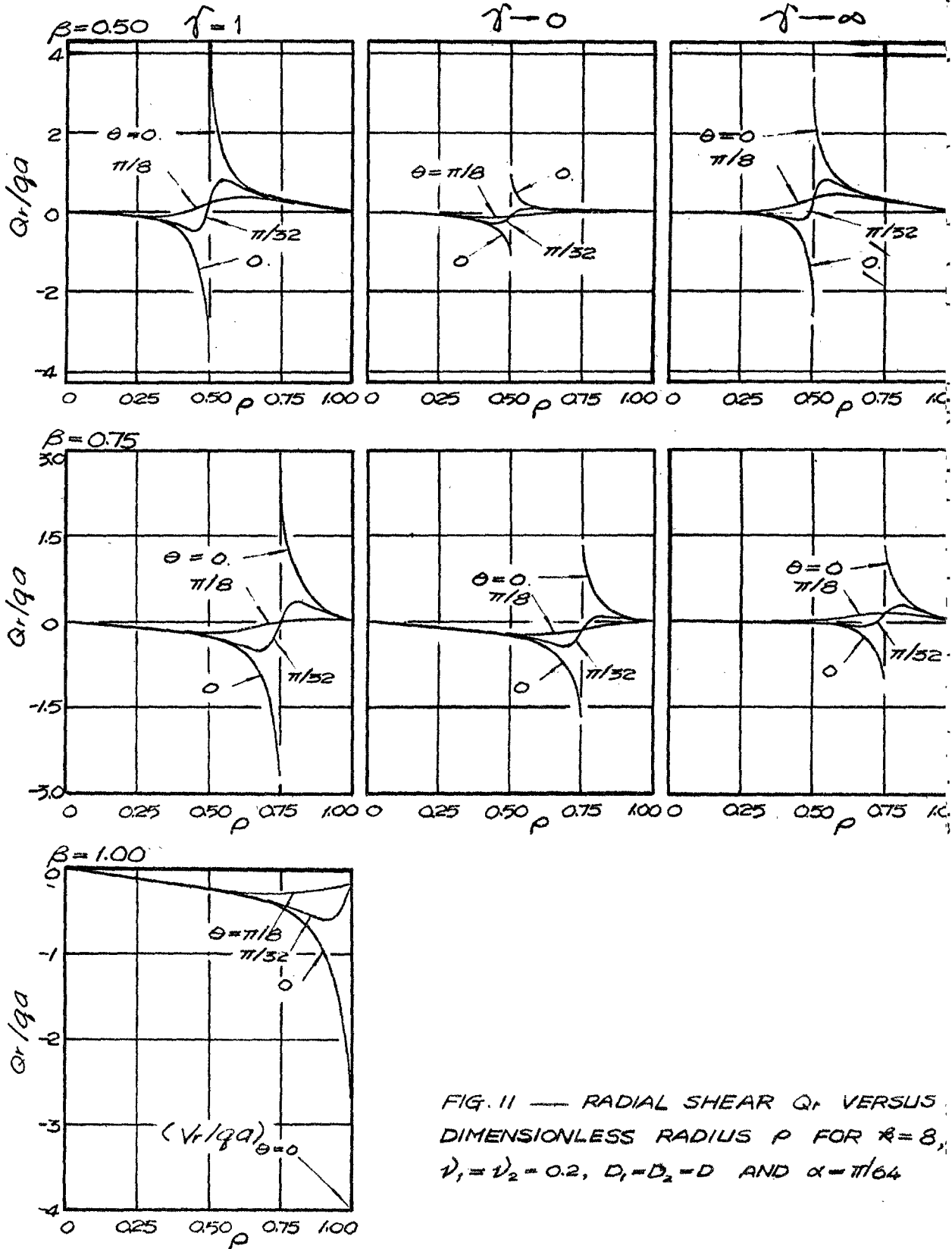


FIG. 11 — RADIAL SHEAR  $Q_r$  VERSUS  
DIMENSIONLESS RADIUS  $p$  FOR  $\kappa = 8$ ,  
 $\nu_1 = \nu_2 = 0.2$ ,  $D_1 = D_2 = D$  AND  $\alpha = \pi/64$

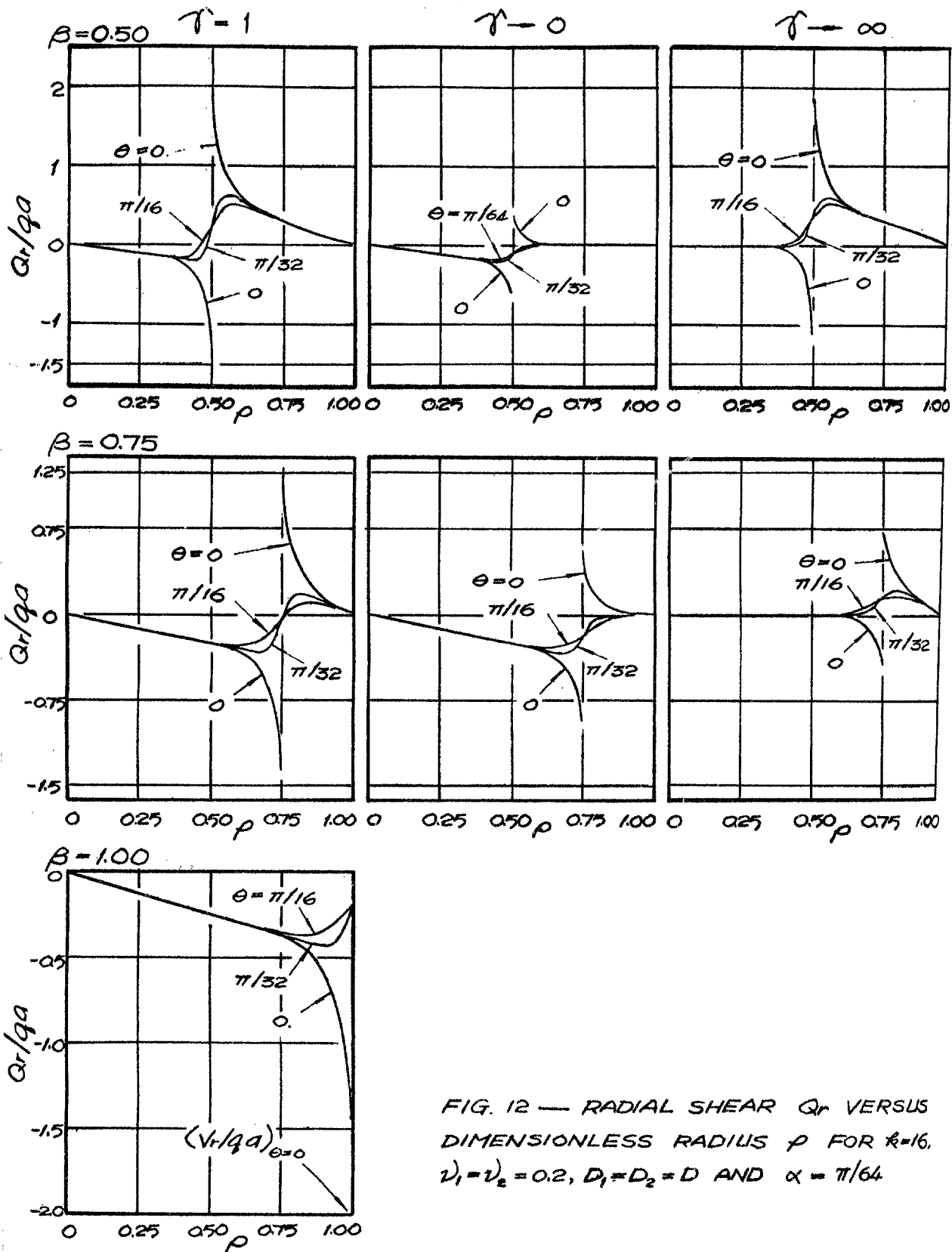


FIG. 12 — RADIAL SHEAR  $Q_r$  VERSUS  
DIMENSIONLESS RADIUS  $\rho$  FOR  $k=16$ ,  
 $v_1=v_2=0.2$ ,  $D_1=D_2=D$  AND  $\alpha=\pi/64$

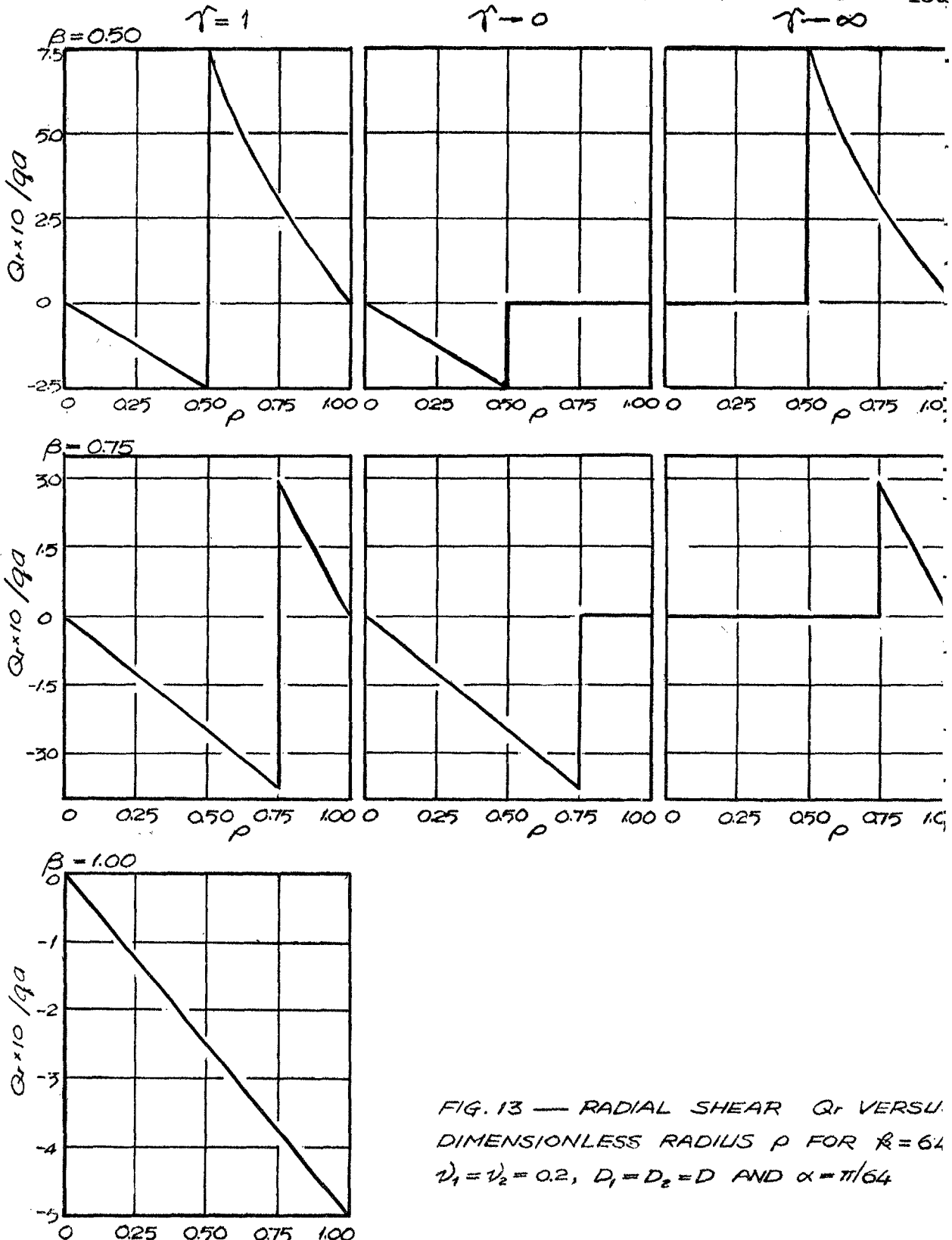


FIG. 13 — RADIAL SHEAR  $Q_r$  VERSUS  
DIMENSIONLESS RADIUS  $\rho$  FOR  $R = 64$   
 $\nu_1 = \nu_2 = 0.2$ ,  $D_1 = D_2 = D$  AND  $\alpha = \pi/64$

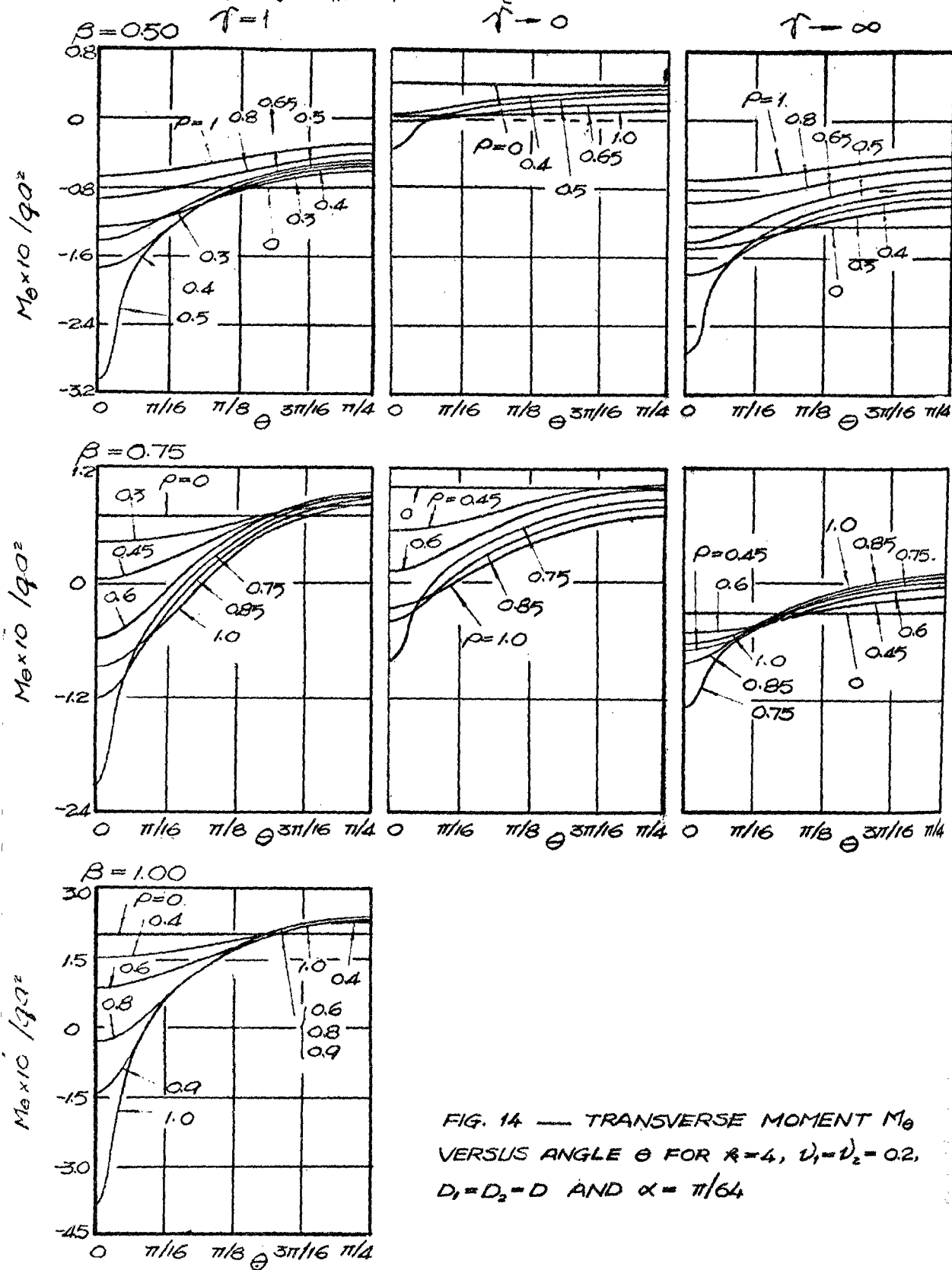


FIG. 14 — TRANSVERSE MOMENT  $M_\theta$   
VERSUS ANGLE  $\theta$  FOR  $R=4$ ,  $V_1=V_2=0.2$ ,  
 $D_1=D_2=D$  AND  $\alpha=\pi/64$

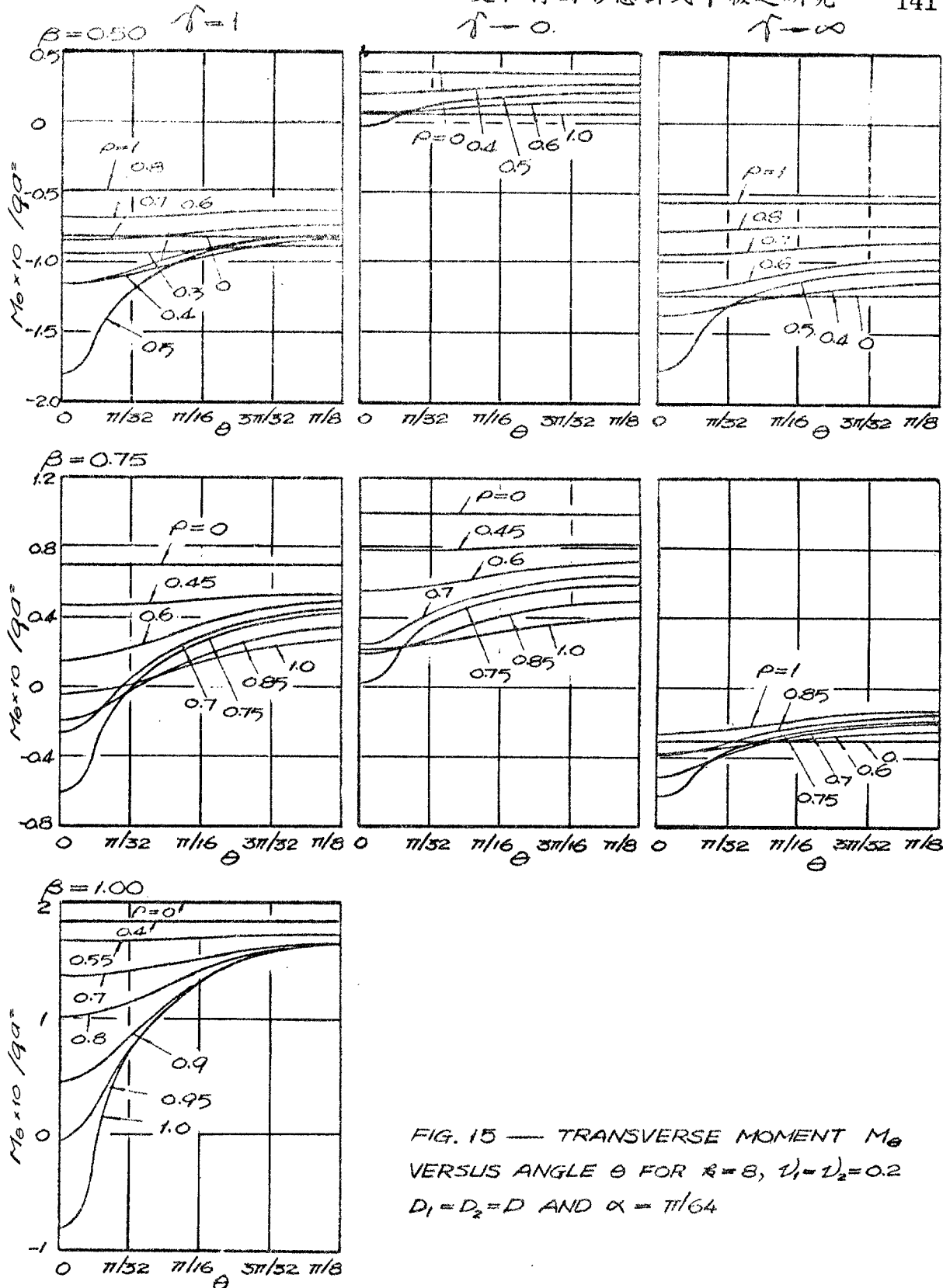


FIG. 15 — TRANSVERSE MOMENT  $M_\theta$   
VERSUS ANGLE  $\theta$  FOR  $R=8$ ,  $V_1=V_2=0.2$   
 $D_1=D_2=D$  AND  $\alpha=\pi/64$

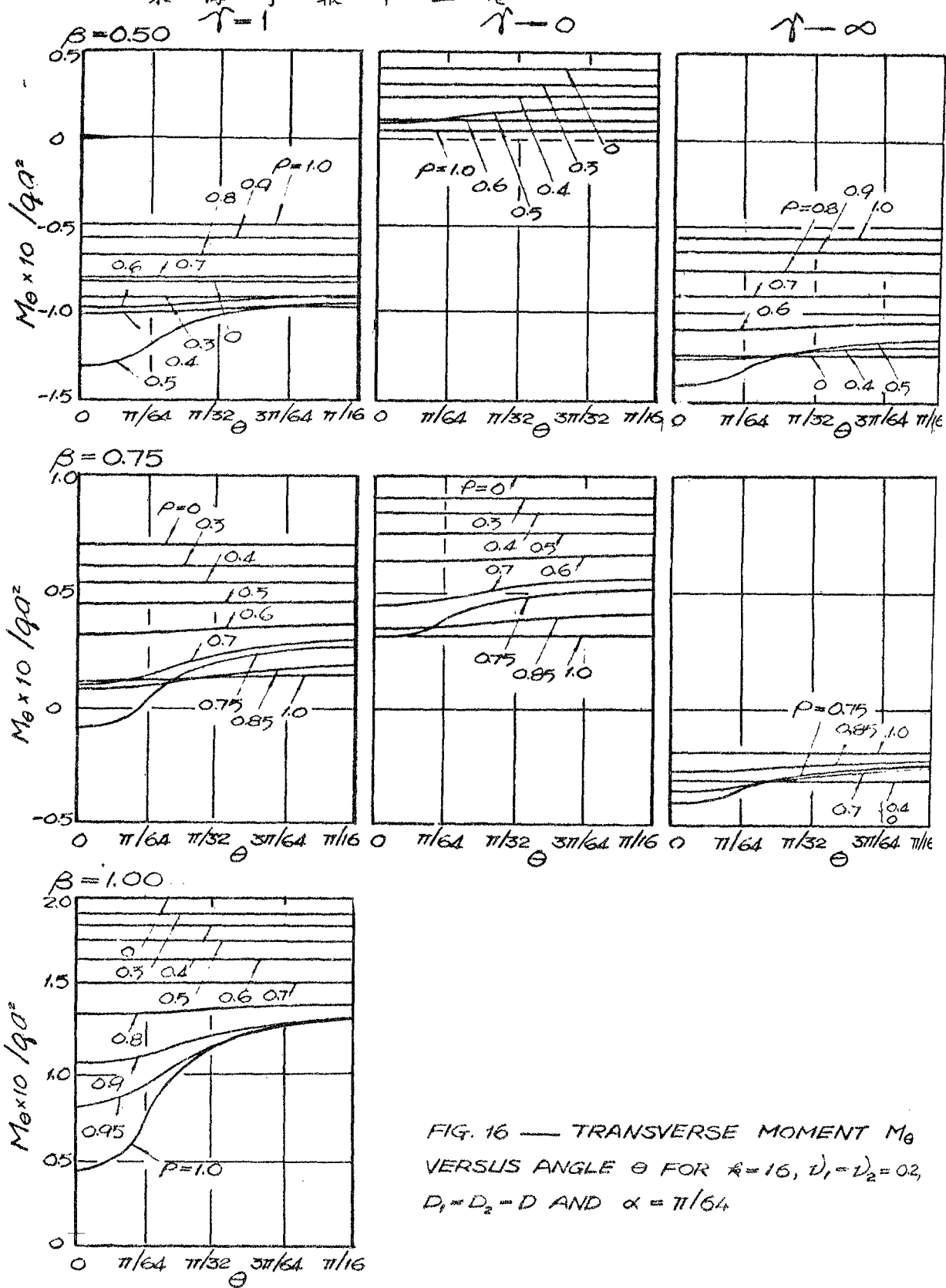


FIG. 16 — TRANSVERSE MOMENT  $M_\theta$  VERSUS ANGLE  $\theta$  FOR  $R = 16$ ,  $D_1 = D_2 = 0.2$ ,  $D_1 = D_2 = D$  AND  $\alpha = \pi/64$

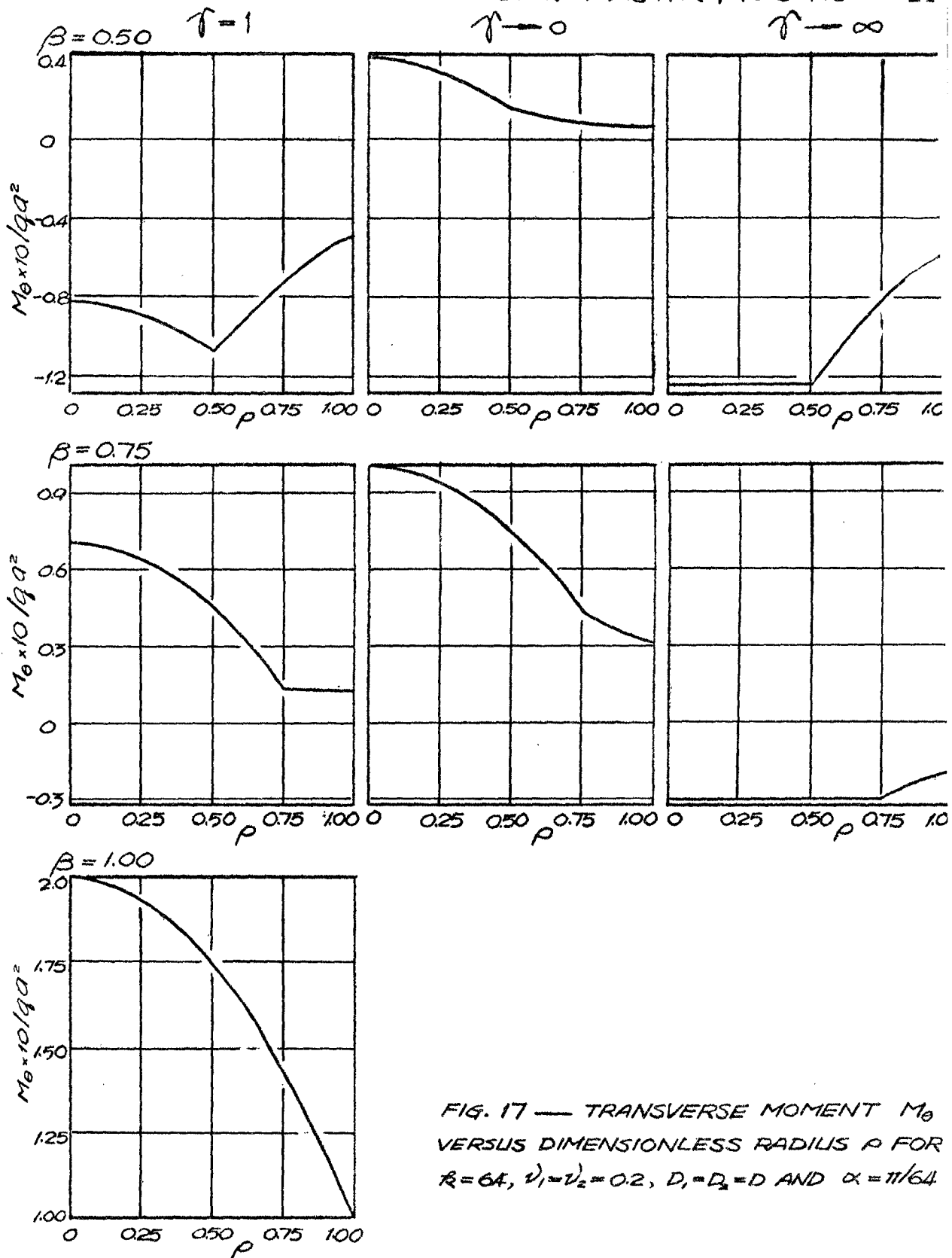


FIG. 17 — TRANSVERSE MOMENT  $M_\theta$  VERSUS DIMENSIONLESS RADIUS  $\rho$  FOR  $R=64$ ,  $\nu_1=\nu_2=0.2$ ,  $D_1=D_2=D$  AND  $\alpha=\pi/64$

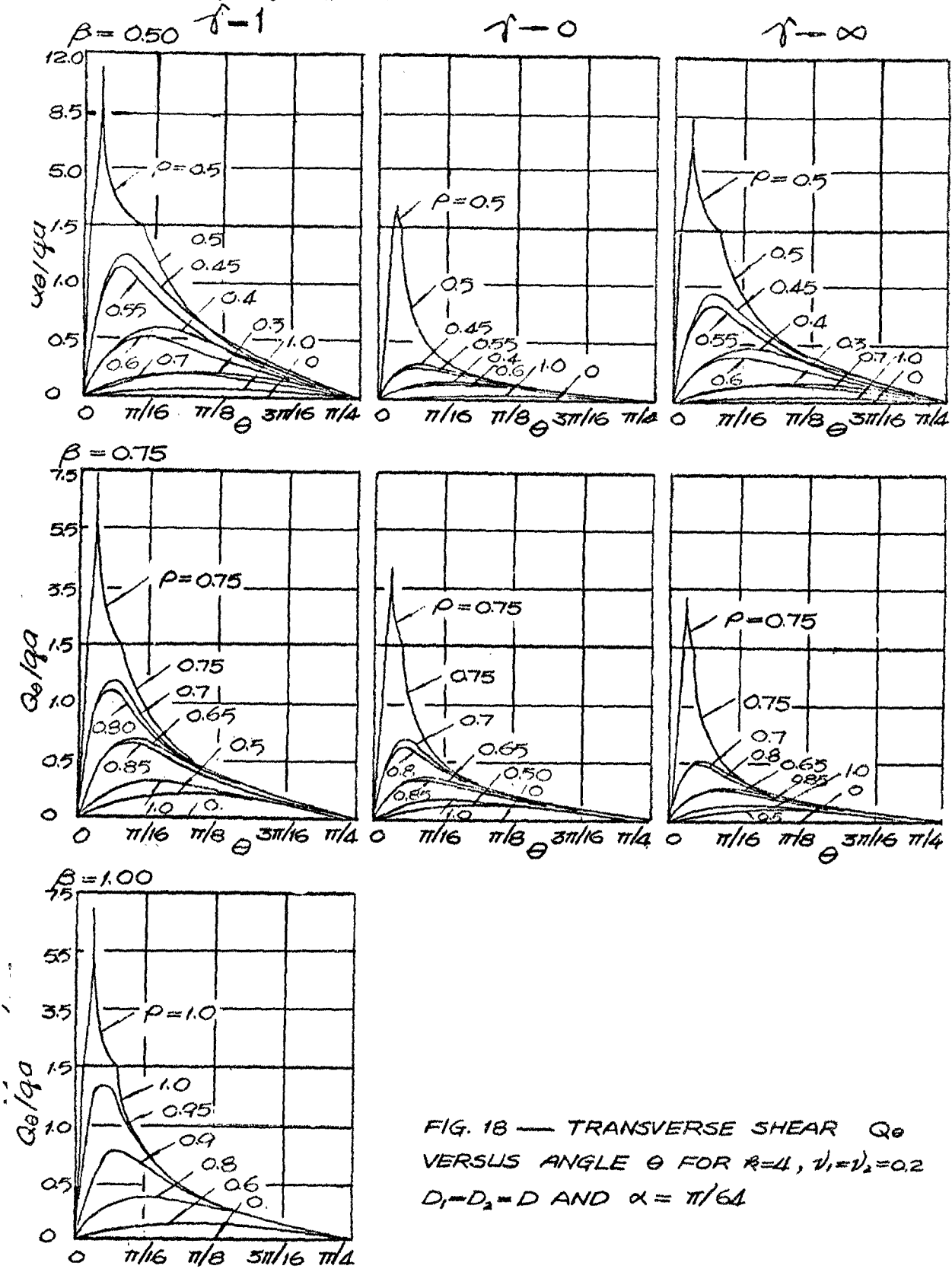


FIG. 18 — TRANSVERSE SHEAR  $Q_\theta$   
VERSUS ANGLE  $\theta$  FOR  $R=11$ ,  $\nu_1=\nu_2=0.2$   
 $D_1=D_2=D$  AND  $\alpha = \pi/64$

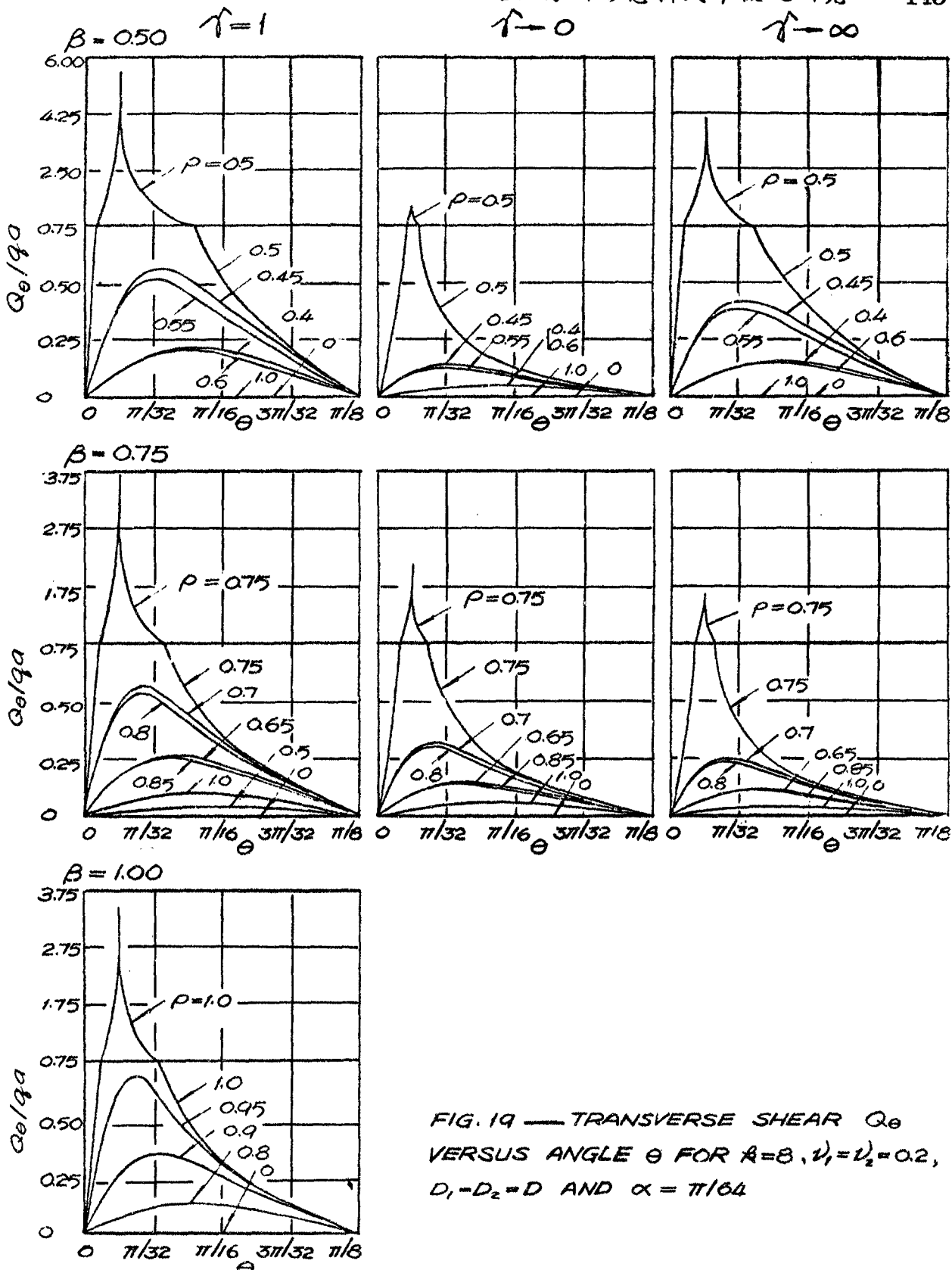


FIG. 19 — TRANSVERSE SHEAR  $Q_\theta$  VERSUS ANGLE  $\theta$  FOR  $A=8$ ,  $V_1=V_2=0.2$ ,  $D_1-D_2=D$  AND  $\alpha=\pi/64$

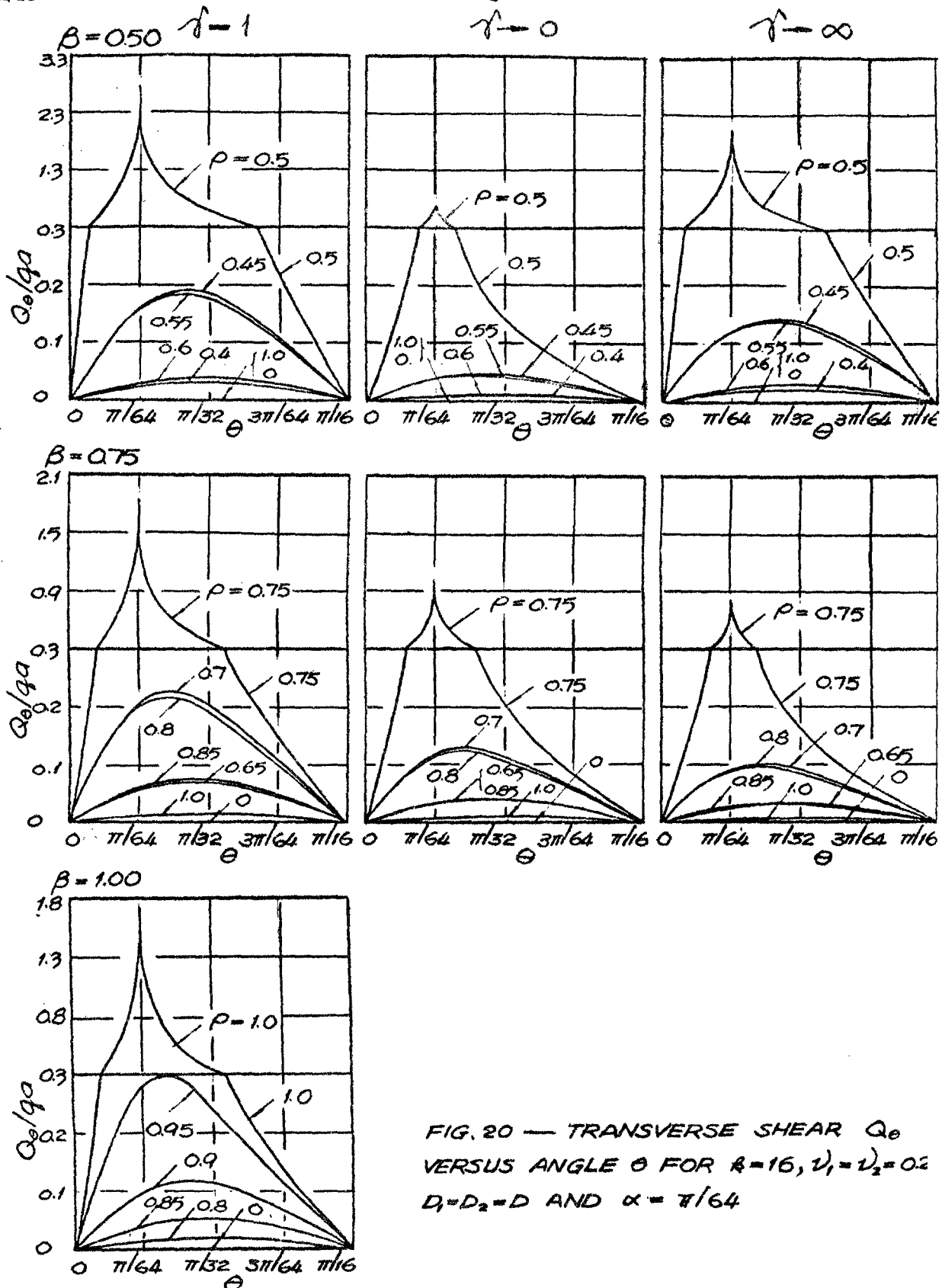


FIG. 20 — TRANSVERSE SHEAR  $Q_\theta$   
VERSUS ANGLE  $\theta$  FOR  $R=16$ ,  $V_1=V_2=0.2$   
 $D_1=D_2=D$  AND  $\alpha=\pi/64$